Nanomechanics of the giant protein titin

PhD thesis

Zsolt Mártonfalvi

Doctoral School of Basic Medicine
Semmelweis University

Supervisor: Dr. Miklós Kellermayer M.D., D.Sc.

Official reviewers:
Dr. Miklós Geiszt M.D., D.Sc.
Dr. Mihály Kovács, D.Sc.

Head of the Final Examination Committee:
Dr. Pál Röhlich M.D., D.Sc.

Members of the Final Examination Committee:
Dr. Ferenc Vonderviszt, D.Sc.
Dr. Zoltán Benyó M.D., D.Sc.

Budapest
2014

Introduction

Titin (also known as connectin) forms an integrating, filamentous scaffold system within the skeletal and cardiac muscle. It spans the distance between the middle and the edge of the sarcomere and is tightly bound in the Z-disk, the M-line and the thick filament. The molecule is a linear chain of globular (immunoglobulin or Ig and fibronectin or FN) domains interrupted with unique sequences such as the unstructured PEVK domain. Alternative splicing that affects mainly the I-band section results in tissue-specific size isoforms which differ in the number of the Ig-domains and the size of the PEVK domain. Whereas nearly 2200 amino acid residues make up the PEVK domain in the largest skeletal-muscle isoform (*m. soleus*), the N2B cardiac titin isoform contains merely 163. Due to its arrangement within the sarcomere, titin is particularly well localized to sense the stress and strain the sarcomere is exposed to. Therefore, it has been proposed that titin might act as a key mechanosensor protein in muscle. The complex array of its potential interaction partners, among which even nuclear proteins may be found, lend support to titin's mechanosensory role. However, the molecular mechanisms behind the possible mechanosensor function of titin are not known.

A mechanosensor function requires that the molecule be exposed and react to local forces. The response of titin to mechanical forces has been quite extensively studied in single-molecule experiments. The current model of *in situ* titin extensibility suggests a hierarchical extension based on the different local persistence length of the various segments and domains within the molecule's I-band section. At low forces the tandem-Ig regions elongate, driven by straightening of the inter-domain linkers. At higher forces the PEVK domain is recruited into the elongation process, providing a continuous extensibility due to its putative random structure. Finally, the unique sequence in the N2B provides additional extensibility, at least in cardiac muscle. Even though globular domains are expected to unfold at increasing passive forces according to transient-state theory, immunolabeling studies, in which the equilibrium fractional extension of titin's segments can be identified at various sarcomere lengths, have typically failed to demonstrate significant levels of unfolding. Such events may be evoked only beyond physiological circumstances. Mechanosensing requires, in addition, that titin's properties somehow reflect the temporal and spatial features of mechanical exposure. Accordingly, the contractile history of the sarcomere is expected to influence the mechanical properties of titin. We have previously shown that the mechanical response of titin wears out in repeated stretch-relaxation cycles, resulting in a mechanical fatigue of the molecule. The

molecular detail and the possible role of this process, however, remained elusive. The lack of precise knowledge about the physiologically relevant force range to which a single titin molecule is exposed to within the sarcomere makes it difficult to sort out the potential mechanosensory mechanisms. At present it is hypothesized that the force per titin in the physiological sarcomere length range is small (approximately 0-20 pN), and in this force regime the titin molecule is thought to behave as a purely entropic chain more or less devoid of internal interactions. In spite of this, if a relaxed sarcomere is exposed to rapid stretch within this sarcomere-length range, passive force decays spectacularly after an initial peak. The mechanisms of this titin-dependent stress-relaxation process are still debated.

Objtectives

Our aim with this work was to investigate force driven the structural transitions in single titin molecules, particularly in the physiological low-force regime. Our objectives were:

1. To isolate individual native titin molecules from rabbit skeletal and cardiac muscle
2. To mechanically manipulate single titin molecules with optical tweezers in order to reveal the molecules force spectrum at the physiologically relevant low-forces.
3. To characterize the low-force stretch transitions.
4. To reveal the underlying structural elements responsible for the low-force transitions.
5. To investigate the dynamics of the low-force transitions.
6. To stretch individual titin molecules with receding meniscus.
7. The topographical analysis of the surface adhered molecules.

Methods

Isolation of native titin molecules

Native titin molecules were isolated from rabbit (*Oryctolagus cuniculus, New Zealand White*) according to our group's previously established protocols. Cardiac-muscle titin was prepared from rabbit myocardium *via* steps identical to those of the skeletal-muscle titin purification procedure but with buffer volumes scaled down according to initial tissue mass. Use of rabbit as the source of specimen was approved by the Regional Ethics Committee (Approval number: XIV-I-001/29-7/2012).

Single molecule manipulation

For nanomanipulation, the Z-line end of titin was captured with a 3.0 μm carboxylated latex bead coated with the T12 anti-titin antibody. The other bead used was a 2.5 μm amino-modified latex bead coated with the photoreactive cross-linker sulfo-SANPAH, providing a non-sequence-specific covalent linkage. Buffer condition for the measurements was 25 mM imidazole-HCl (pH 7.4), 200 mM KCl, 4 mM $MgCl_2$, 1mM EGTA, 1mM DTT, 20 μg/ml leupeptin, 10 μM E-64, 0.1 % NaN. One of the beads was captured in the optical trap, whereas the other one was held with a micropipette embedded in a custom-built flow chamber mounted on a close-loop piezoelectric (PZT) stage. Nanomechanical manipulation of titin was carried out with a custom-built dual-beam counter-propagating optical tweezers apparatus in either constant velocity (velocity-clamp) or constant force (force-clamp) mode (**Figure 1**).

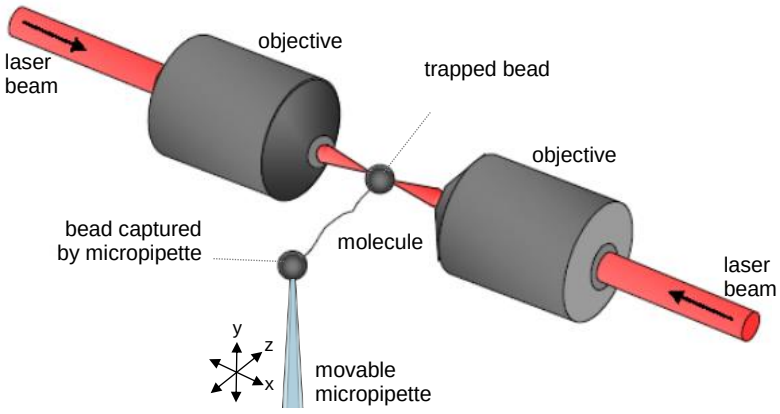

Figure 1 *Double beam optical tweezers. Two counter propagating laser beams form the optical trap. The molecule is captured via surface functionalized microbeads. The mechanical manipulation is controlled by the movable micropipette.*

In order to mount a titin molecule by both of its ends to either of the beads, the pipette-bead, coated with sulfo-SANPAH, was gently pressed against the trapped bead carrying titin via the T12 antibody epitope until a tether was established. Because the binding of the bead coated with sulfo-SANPAH is not sequence-specific, the binding location was calculated *a posteriori,* based on the molecule's nanomechanical behavior.

Titinmolekulák nyújtása folyadék meniszkusszal

Titin was extended by molecular combing with receding meniscus based on steps reported earlier (**Figure 2**). Titin was diluted with PBS solution (10 mM K-phosphate pH 7.4, 140 mM NaCl, 0.02% NaN_3) containing 50% glycerol to an approximate final protein concentration of 20 mg/ml. In typical experiments urea was added to a final concentration of 1 M to reduce protein aggregation. At this concentration urea was shown not to induce globular-domain unfolding. 20 ml sample was applied to freshly cleaved mica and immediately spun in a custom-built rotor with 13,000 RPM for 10 s. Following spinning, but before the complete drying of the residual liquid layer, the mica surface was extensively washed with distilled H_2O and dried with clean N_2 gas. Often the specimen was dried further under ambient conditions prior to AFM imaging. In some experiments the sample was covered with PBS solution immediately after the centrifugation step so as to reveal molecular structure unaffected by dehydration.

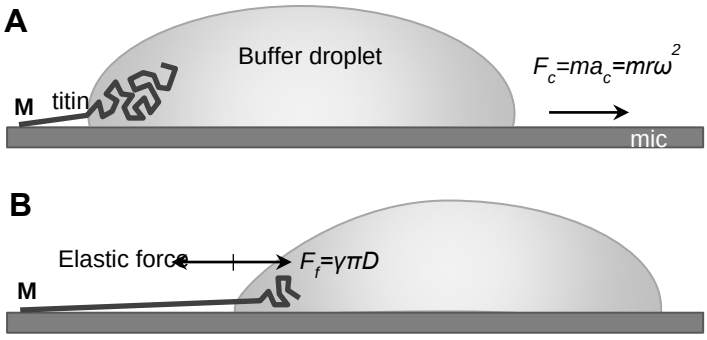

Figure 2 *Stretching titin with receding meniscus.* ***A:*** *A titin molecule, attached by one of its ends (typically its M-line end, indicated with M) to the mica surface is pulled by a receding buffer droplet accelerated by centrifugal force (F_c). m is droplet mass and r is the distance from the center of* ***B:*** *At each time point during droplet movement, a surface-tension($_C$)-based force (F_{st}, counteracted by the elastic force borne in the protein chain), proportional to chain diameter (D), stretches titin before it is stabilized by binding to the surface.*

Results

Single molecules of native, full-length titin purified from rabbit skeletal and cardiac muscles were manipulated in the present work, by using optical tweezers, with the objective of resolving mechanically-driven structural changes across physiologically relevant force and temporal scales. Force *versus* extension data obtained in constant-velocity experiments on rabbit *m. longissimus dorsi* titin is shown in **Figure 3**.. During stretch, transitions which extend the molecule progressively, begin appearing already below 20 pN. The sharp, discrete transitions continued to occur until the end of the stretch half-cycle. However, the spacing between the transitions, which corresponds to the contour-length gain of the titin chain caused by the transition, appear to be different below approximately 40 pN than above this force value even by visual assessment. Whereas above 40 pN the transitions are more-or-less evenly spaced by about 30 nm, below 40 pN there is a large variation in contour-length gain, and large (several hundred nm) contour-length-gain steps also appeared.

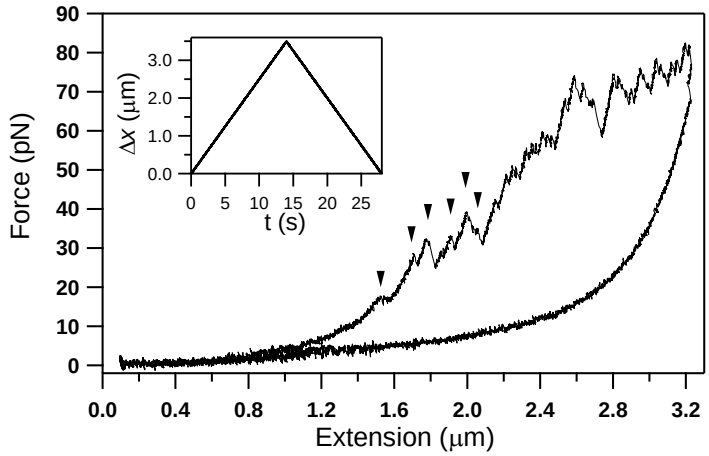

Figure 3 *A complete stretch-relaxation cycle of skeletal muscle titin. Arrows indicate discrete low-force transitions. Inset shows piezo displacement (Δx) during experiment.*

The contour-length gain upon the transitions was calculated by fitting the rising half of the force sawtooth with the wormlike-chain equation and subtracting the contour length values resulting from the fit for every neighboring transition. The transition forces were obtained by recording the instantanous force at the moment of the transition (sawtooth peak). From the scattergram of contour-length gain (ΔL_C) *versus* transition force (**Figure 4A**) a partitioned ΔL_C distribution emerged. In case of the skeletal titin isoform, above ~40 pN a major peak centered at 30 nm (31.7 ± 5.3 nm S.D.) and a minor peak centered at 60 nm were observed. By contrast, below ~40 pN a major peak ranging between 10-80 nm and centered

around 30 nm dominated the otherwise very wide distribution of the dataset. In case of the cardiac titin isoform, the contour-length-gain distribution contained a major peak centered at 30 nm (28.6 ± 4.5 nm) and a minor peak at 60 nm, and ΔL_C was broadly distributed below 40 pN (**Figure 4B**). However, the overall ΔL_C distribution was much narrower than in the case of the skeletal isoform. Such differences of the two isoform may be due to the different length of

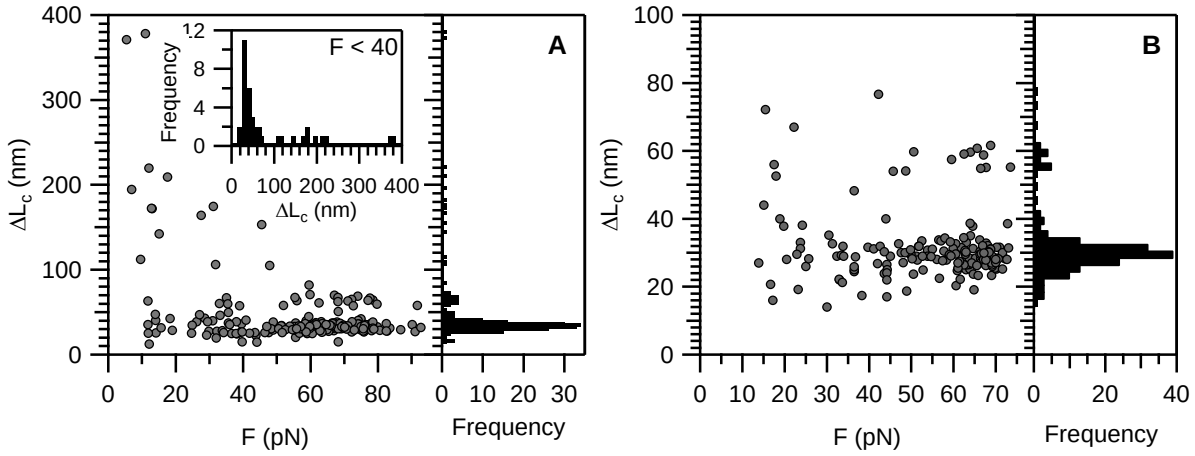

Figure 4 *Scatter plot of contour-length displacement (ΔL_c) as a function of transition force ($F_{transition}$) for different titin isoforms.* ***A:*** *Skeletal muscle isoform. Inset shows ΔL_c histogram at forces below 40 pN.* ***B:*** *Cardiac isoform.*

the PEVK domains. To further test for this option we designed experiments in which we passivated the PEVK domain by the sequence specific 9D10 antibody. To completely exclude the role of the PEVK domain, we manipulated titin by grabbing it with beads coated with the T12 and 9D10 antibodies. In these experiments we thus manipulated the proximal tandem-Ig and N2A regions of titin. The transitions extended the contour length of the molecule by 30 nm on average (**Figure 5**), suggesting that Ig-domain unfolding exclusively determined the

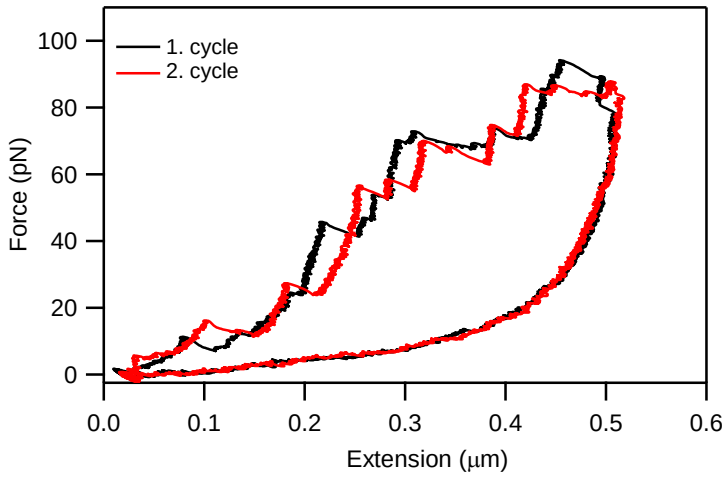

Figure 5 *Stretching titin with T12 and 9D10 coated beads to completely inactivate the PEVK domains contribution to mechanics. 10 second pause between consecutive cycles.*

nanomechanical behavior of this titin tether. The force hysteresis completely recovered during the 10-s pause in the contracted state between the mechanical cycles.

To assess the rate of extension at low forces, constant-force experiments were carried out. Titin was stretched to a predetermined set-force value, and the extension of the molecule was varied rapidly so as to maintain the force level constant. Even at low clamp forces the molecule extended in well discernible steps. We varied the clamp force so as to gain access to the spontaneous transition rate. The time-dependent extension traces were fitted with double-exponential functions, and the force-dependent rate constants were calculated for both the fast and the slow component of the stepwise extension process (**Figure 6**).

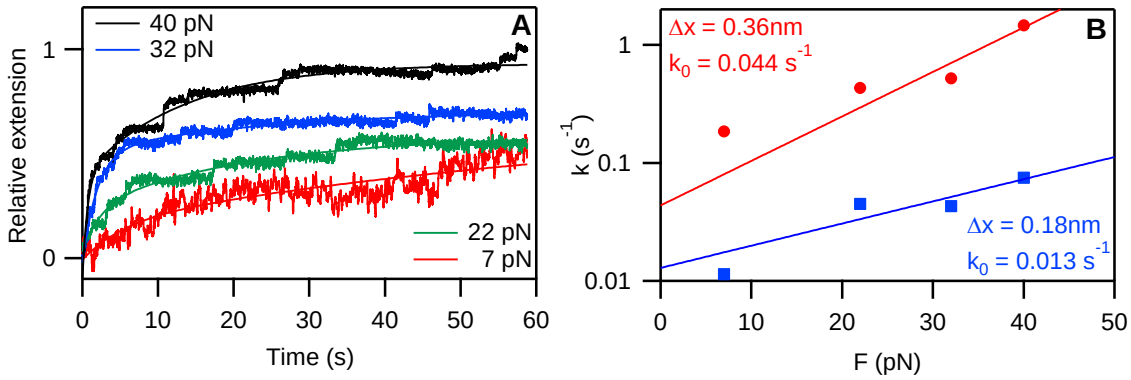

Figure 6 *Stretching titin with force feedback optical tweezers.* ***A:*** *Extension curves at different clamp forces fitted with double exponential.* ***B:*** *rate constants obtained from the fits and fitted with the modified Bell model equation. Red: slow component, blue: fast component.*

From the load-dependent rate constants we calculated the spontaneous rates of the stepwise extension based on the modified Bell's modell equation: for the fast component we obtained a spontaneous rate (k_0) of 0.044 s^{-1}, and for the slow component k_0 was 0.013 s^{-1}. The distance, along the reaction coordinate, from the contracted to the transition states (Δx) was 0.36 nm and 0.18 nm for the fast and slow components, respectively.

To investigate the potential biological significance of the low-force transitions and their role in titin's mechanical fatigue, we carried out stretch and relaxation experiments in complex patterns. First, titin was stretched in successive mechanical cycles, with no pause between the cycles, followed by a probe stretch after a 10 second pause. Force hysteresis could be recovered upon resting the molecule in the contracted state. Whereas the hysteresis recovered partially during a 10-s resting pause (**Figure 7**), it recovered after 20 s. Thus, the time spent in a distinct contraction state (i.e., fixed extension) significantly influences the force pattern in the next mechanical cycle.

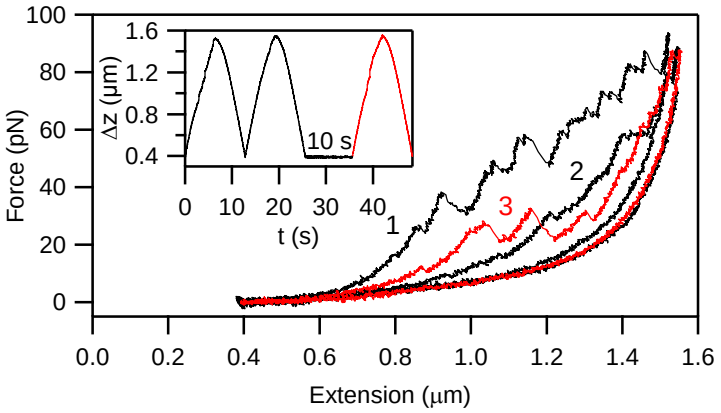

Figure 7 *Effect of slack pause time on titin's fatigue. A skeletal-muscle titin molecule was manipulated in two immediately successive stretch-relaxation cycles (stretch rate 250 nm/s) followed by a rest period of 10 s, then by a third, monitoring stretch relaxation cycle. Inset shows the end-to-end distance change of the molecule.*

To investigate how the contraction state influences titin's mechanical fatigue, we stretched a single molecule with constant, 250 nm/s velocity to an extension of 2.8 μm, then rapidly quenched the extension to different end-to-end lengths 743 nm and paused for 20 s. Subsequently, the molecule was stretched in a complete mechanical cycle with 250 nm/s velocity (**Figure 8**). Upon increasing the resting end-to-end length of the molecule, the probability of recovering the force hysteresis gradually decreased, and the initial stretch force curve became progressively shifted to increasing extensions. The overall pattern of the high-force transitions (>40 pN), judged from the sequence of the sawtooth force peaks, however, remained similar while being shifted right (to high extensions). Thus, most of the globular

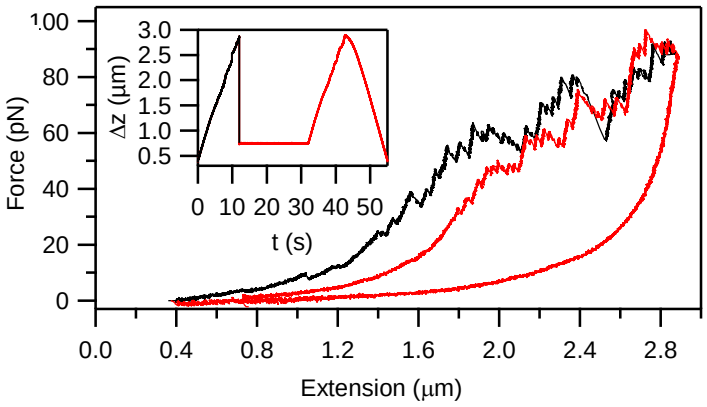

Figure 8 *Effect of contractile status on titin's fatigue. The skeletal-muscle titin molecule was first stretched, at a constant rate of 250 nm/s, to an extension of ~2.8 μm, then the extension was rapidly quenched for 20 s to 743 nm, then a complete stretch-relaxation cycle was carried out. Inset shows the end-to-end distance change of the molecule.*

domains unfolded during the first mechanical cycle refolded during the 20-s rest period in all cases, whereas the intramolecular interactions behind the low-force transitions failed to be reestablished if the end-to-end length of titin was increased, and the stretch curve of the second mechanical cycle was highly sensitive to the resting extension of the titin molecule.

Titin's history-dependent mechanical behavior may serve as a mechanosensor only if information is relayed towards signal-transduction pathways, which are typically cascades of molecular recognition and binding. Conceivably, the low-force structural transitions in titin change the exposure of sites to phosphorylation and the binding of ligands. The mechanical opening of cryptic binding sites in multimodular proteins is thought to be an important mechanosensory mechanism, that may take place in titin.

To further investigate the force driven structural changes in titin, molecules, prepared from rabbit *m. longissimus dorsi*, were stretched by molecular combing with receding meniscus and their topographical structure was analyzed with AFM (**Figure 9**). The topographical structure of extended titin molecules was studied in height contrast images. Gaps were discerned along the axis of the overstretched titin that interrupted its contour, and which were distributed more or less evenly along the molecule. Occasionally we resolved fine filamentous structures within the gaps.

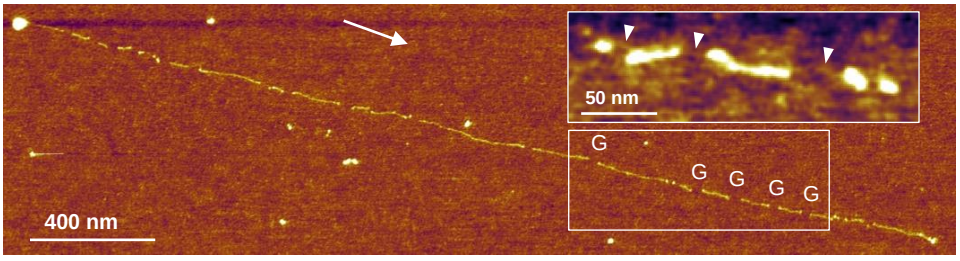

Figure 9 *Topographical analysis of overstretched titin molecules by molecular combing. Contour gaps in the molecule are shown with G. Arrow indicates the direction of meniscus movement.* **Inset:** *Fine structure of contour gaps. Arroe indicate thin filamentous structures spanning the gap.*

Conclusions

Low-force structural transitions in titinI

In the present work we mechanically manipulated individual titin molecules from rabbit *longissimus dorsi* and cardiac muscles by exposing them to complex tests with high-resolution optical tweezers. In velocity-clamp stretch-relaxation experiments carried out at 250 nm/s stretch rate discrete, sawtooth-shaped transitions appeared during stretch, which extended the contour length of the molecule in a stepwise manner. Above ~40 pN, the sawtooth-shaped transitions extend the molecule by ~30 nm on average in both skeletal and cardiac titin, therefore these transitions are identified as all-or-none globular domain unfolding events.

Experiments in which only the proximal tandem-Ig region of titin was manipulated demonstrate that this segment of the molecule indeed contains a few (2-3) domains that unfold below 40 pN. The precise allocation of these mechanically unstable domains to the sequence and domain structure of titin requires further experimentation. In the sub-40-pN transition-force range the ΔL_c distribution became wide (ten to several hundred nm), indicating that the sudden steps of contour-length increment are not solely due to the unfolding of globular domains, but additional force-bearing conformations and interactions between remote, structurally less specific binding sites of the titin chain also contribute to the mechanical behavior.

It is plausible to hypothesize that the PEVK domain contributes significantly to the appearance of the discrete transitions, even though previously we haven't been able to detect such steps most likely due to low force and time resolution. During molecular fatigue the rupture of intrachain bonds extends the contour-length of titin during stretch, but the bonds are unable to recover on a short time scale; therefore, the process manifests in a progressive shift of the stretch force curve towards increasing extensions and a corresponding reduction in force hysteresis. Our current high-resolution measurements also revealed the molecular fatigue phenomenon and indicate that both regularly- and irregularly-spaced sawtooth-shaped force transitions, corresponding to globular-domain unfolding and conceivably to bond rupture or unfolding of transient structures within the PEVK domain, respectively, contribute to the process.

We hypothesize that two types of structural transitions may occur in PEVK in response to stretch: unfolding of low-energy conformations (polyproline helices, ß-turns)

present in the 28mer repeat units and rupture of electrostatic interactions between more distant, oppositely charged regions. While the re-establishment of the former is inhibited at low ionic strength due to electrostatic stiffening, the latter is present even at low ionic strengths. Altogether, in the low-force-regime mechanics of the titin molecule both the stepwise extension of the PEVK and the unfolding of low-stability globular domains are manifested, and in a given force response the structural transitions caused by either of these processes follow each other randomly.

Our findings indicate that the force *versus* extension response of titin reflects the recent history of the mechanical conditions to which the molecule has been exposed. By sensing the mechanical environment and providing a suitably modified force response titin fulfils a mechanosensor function. The mechanical parameters that influence the force response are force, space and time. Accordingly, titin's stretch force curve is sensitive to prior loads and loading rates, the prior end-to-end distance at which it was held, and the time spent in a given configuration. The response function is a history-dependent change in the effective contour length, which manifests in a shift of the force trace along the extension axis. Progressive shift towards increasing or decreasing extensions corresponds to molecular fatigue or mechanical recovery, respectively. Our results indicate that a dual molecular mechanism is responsible for the mechanosensitive response: the PEVK domain and a few unstable domains in the proximal tandem-Ig region.

Stretching titin with receding meniscus

Molecular combing has been successfully applied for the investigation of overstreched titin molecules. The structural hallmarks of globular-domain unfolding were investigated by topographical analysis of high-resolution (0.5– 2 nm pixel resolution) AFM images. We observed distinct gaps in the titin filaments that interrupted the axial contour. A gap was hereby defined as an axial interruption the bottom of which is in plane with the substrate surface. The average gap width was 27.7 nm, which compares well with the contour length of an unfolded globular domain in titin. Thus, the gaps are the apparent morphological manifestations of individual domain unfolding events, further supporting the notion that domains unfold independently upon the action of mechanical force.

New scientific results

I. Titin extends via discrete steps even at low forces (5 pN < F < 40 pN) due to force-driven structural changes of the molecule.

II. The low force structural transitions are caused both by the unfolding of mechanically weak globular domains and the rupture of transient structures and electrostatic interactions of the PEVK domain.

III. Low force transitions contribute to titin's mechanical fatigue. Their pattern and recovery rate reflect the molecule's contractile history.

IV. Force driven domain unfolding and PEVK extension can be visualized by topographical analysis of individual titin molecules stretched with receding meniscus.

V. The width of the first contour gap, likely to be the kinase domain, located at the C-terminal, M-line end of the meniscus stretched molecules is proportional to the stretch force.

Publications related to the PhD thesis

Mártonfalvi Z, Bianco P, Linari M, Caremani M, Nagy A, Lombardi V, Kellermayer M. (2014) Low-force transitions in single titin molecules reflect a memory of contractile history. J Cell Sci, 127:858-870. IF: 5.877

Mártonfalvi Z, Kellermayer M. (2014) Individual Globular Domains and Domain Unfolding Visualized in Overstretched Titin Molecules with Atomic Force Microscopy. PLoS One, 9:e85847. IF: 3.733